Current Biology 25, 175–186, February 2, 2015 http://dx.doi.org/10.1016/j.cub.2014.11.043

Article

Rac1-Dependent Phosphorylation and Focal Adhesion Recruitment of Myosin IIA Regulates Migration and Mechanosensing

Ana M. Pasapera,[1] Sergey V. Plotnikov,[1,2] Robert S. Fischer,[1] Lindsay B. Case,[1] Thomas T. Egelhoff,[3] and Clare M. Waterman[1,*]

[1]Cell Biology and Physiology Center, National Heart Lung and Blood Institute, National Institutes of Health, Bethesda, MD 20892, USA

[2]Department of Cell and Systems Biology, University of Toronto, Toronto, ON M5S 3G5, Canada

[3]Department of Cellular and Molecular Medicine, Cleveland Clinic Lerner Research Institute, Cleveland, OH 44195, USA

Summary

Background: Cell migration requires coordinated formation of focal adhesions (FAs) and assembly and contraction of the actin cytoskeleton. Nonmuscle myosin II (MII) is a critical mediator of contractility and FA dynamics in cell migration. Signaling downstream of the small GTPase Rac1 also regulates FA and actin dynamics, but its role in regulation of MII during migration is less clear.

Results: We found that Rac1 promotes association of MIIA with FA. Live-cell imaging showed that, whereas most MIIA at the leading edge assembled into dorsal contractile arcs, a substantial subset assembled in or was captured within maturing FA, and this behavior was promoted by active Rac1. Protein kinase C (PKC) activation was necessary and sufficient for integrin- and Rac1-dependent phosphorylation of MIIA heavy chain (HC) on serine1916 (S1916) and recruitment to FA. S1916 phosphorylation of MIIA HC and localization in FA was enhanced during cell spreading and ECM stiffness mechanosensing, suggesting upregulation of this pathway during physiological Rac1 activation. Phosphomimic and non-phosphorylatable MIIA HC mutants demonstrated that S1916 phosphorylation was necessary and sufficient for the capture and assembly of MIIA minifilaments in FA. S1916 phosphorylation was also sufficient to promote the rapid assembly of FAs to enhance cell migration and for the modulation of traction force, spreading, and migration by ECM stiffness.

Conclusions: Our study reveals for the first time that Rac1 and integrin activation regulates MIIA HC phosphorylation through a PKC-dependent mechanism that promotes MIIA association with FAs and acts as a critical modulator of cell migration and mechanosensing.

Introduction

Cell migration is mediated by coupling forces generated in the actin cytoskeleton to integrin focal adhesions (FAs) that adhere to the extracellular matrix (ECM). Nonmuscle myosin II (MII) is the main generator of forces that drive motility [1]. In migrating cells, the two most widely expressed isoforms, MIIA and MIIB, exhibit distinct localizations and functions [2, 3]. MIIB assembles and localizes in the cell center and rear where it promotes front-back polarity and forms a retracting tail [3, 4]. MIIA assembles in the leading edge [5, 6], where it promotes contractile actin arcs [7, 8]. Despite their distinct localizations, both isoforms regulate FA maturation and dynamics. MIIB promotes long-lived FA in the cell center and rear, whereas MIIA promotes maturation and turnover of leading-edge FA [6]. However, MIIs have not been localized to FAs but are thought to act on FAs "at a distance" by transmitting tension through the actin cytoskeleton [9]. Furthermore, how MII is controlled by upstream regulators to specifically modulate FA dynamics during cell migration is not known.

Rac1 is a small GTPase of the Rho family that mediates cell motility, mechanosensing, and invasion [10]. Rac1 activation is promoted by integrin engagement [11, 12], and Rac1 downstream effectors including the p21-activated kinases (PAKs) regulate leading-edge cytoskeletal and FA dynamics [10]. Rac1 promotes actin polymerization to drive protrusion of the leading edge and retrograde flow [13]. In conjunction with lamellipodial protrusion, Rac1 also promotes formation of small FAs near the leading edge [14]. Although leading-edge actin retrograde flow and FA assembly and turnover dynamics are known to be modulated by MII activity [15], it is not known how Rac1 regulates the coordination of F-actin dynamics and adhesion, or whether it is through MII.

The regulation of MII is well studied; however, Rac1's role in this regulation is less clear. Phosphorylation of the MII light chains (MLC) on serine19 (S19) promotes activation of MII ATPase and filament assembly [16, 17]. It is controversial as to whether Rac1 promotes or inhibits cellular contractility via this mechanism in a PAK-dependent manner [18–20]. Phosphorylation of the MII heavy chain (HC) at several sites in the rod and nonhelical tailpiece inhibits MII filament assembly and thus may negatively regulate contractility [21]. Rac1 can promote phosphorylation and redistribution of MII HC via PAK [22, 23]; however, the sites targeted for phosphorylation in MII are not known. Other direct mediators of phosphorylation on MII HC sites include protein kinase C (PKC), TRPM7, and casein kinase II (CKII) [21]. Rac1 can regulate some PKCs indirectly [24], and PKCs are additionally activated by integrin engagement and regulate FA formation [25] and thus are good candidates for mediating the coordination of MII and adhesion in cell migration.

Here, we examined the role of Rac1 in regulation of MII in FA dynamics and cell migration. We find that Rac1 activity promotes capture and assembly of MIIA minifilaments in maturing FA in an integrin-dependent manner. We show that this is mediated by PKC-dependent phosphorylation of serine 1916 on MIIA HC. We demonstrate that this phosphorylation is necessary and sufficient for MIIA recruitment to FA, facilitating rapid FA assembly, enhancing cell migration, and modulating ECM stiffness mechanosensing.

Results

Active Rac1 Promotes MIIA Association with Focal Adhesions

We sought to determine the role of Rac1 activity in MII organization and its role in FA dynamics in the leading edge of

*Correspondence: watermancm@nhlbi.nih.gov

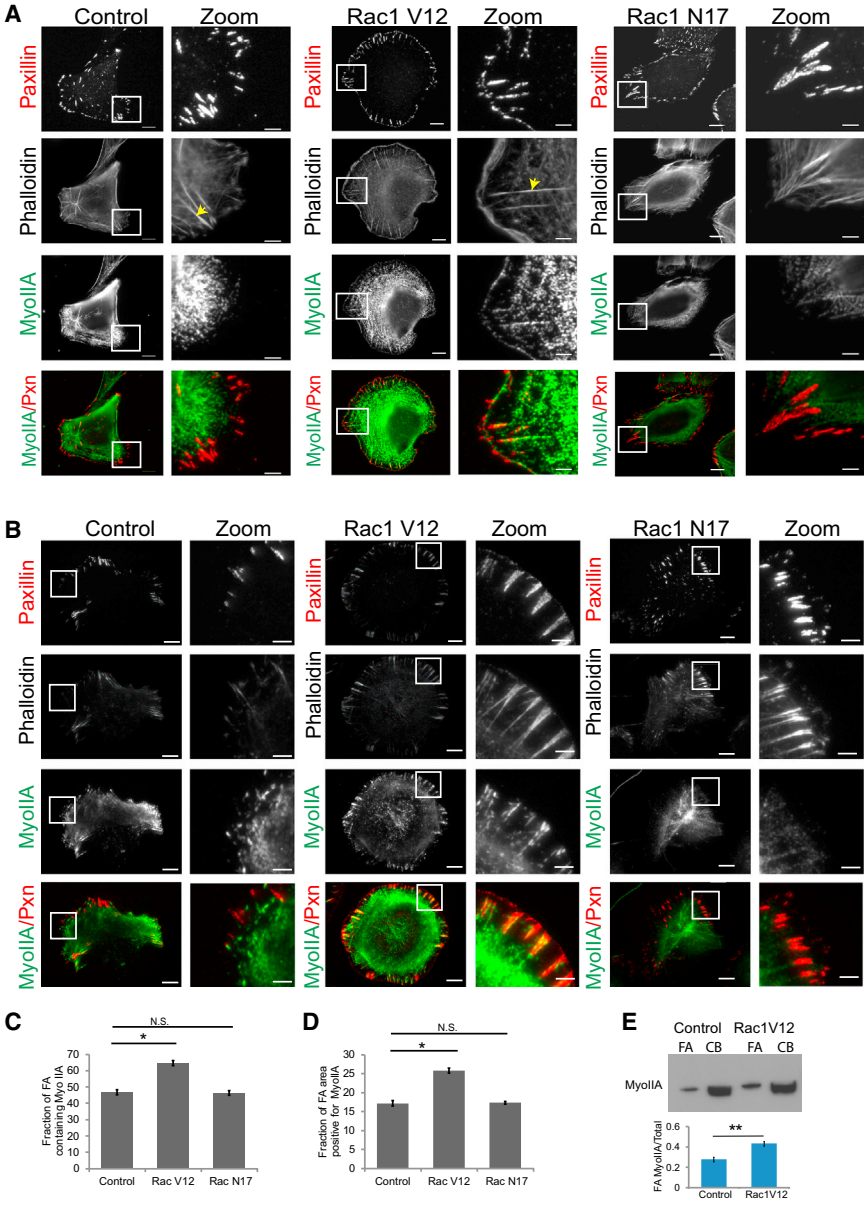

Figure 1. Rac1 Activation Induces Myosin IIA Accumulation at FAs

U2OS without (Control) or with expression of Rac1V12 or Rac1N17 Rac1 mutants immunostained for paxillin (red) and MIIA (green) and actin stained with fluorescent phalloidin.

(A and B) Wide-field epifluorescence (A) and TIRF (B). Zoom, high-magnification of boxed regions. Scale bars, 10 μm in low-magnification images, 3 μm in zoom. (A) Arrowheads, radial SFs.

(C and D) Fraction of FAs that contain MIIA staining. (C) Fraction of FA area co-occupied by MIIA (D) from TIRF images. Control: n = 7 cells; Rac1V12: n = 9 cells; Rac1N17: n = 8 cells; ~100 adhesions/cell.

(E) FA fraction isolated from cell body (CB) fraction in the presence or absence of Rac1V12 expression, western blot with antibodies to MIIA. Quantification of the ratio of MIIA in the FA fraction:total MIIA (FA + CB fractions), n = 3, error bars = SEM; NS (nonsignificant), $p > 0.05$; *$p < 0.05$; **$p < 0.01$.

migrating cells. We utilized human osteosarcoma U2OS cells plated on fibronectin-coated coverslips and transfected with blue fluorescent protein (BFP)-tagged constitutively active (Rac1V12) or dominant-negative (Rac1N17) Rac1 mutants to manipulate Rac1 activity. We immunolocalized MII (either A or B isoforms) and paxillin as a marker of FAs [26] and used fluorescent phalloidin to visualize F-actin and imaged cells by epifluorescence microscopy (Epi). In mock-transfected controls, MIIA was localized along stress fibers (SFs) in the cell center and to actin arcs in the lamella but was absent from lamellipodia, FAs, and radial SFs (Figure 1A), as reported [8, 9, 27]. A similar localization was seen in cells expressing Rac1N17, although lamellipodia were absent (Figure 1A). Expression of Rac1V12 induced a discoid or crescent-shaped morphology with MIIA localized to arcs and SFs in the cell center, similar to controls. However, Rac1V12 caused the additional accumulation of MIIA toward the distal ends of radial SFs that emanated from FAs (Figure 1A). Similar analyses showed that MIIB predominantly localized to SFs in the cell center and rear and was absent from lamellipodia, radial SFs, and FAs, independent of the state of Rac1 activity (Figure S1 available online). Thus, Rac1 activation promotes association of MIIA with SF termini in the lamella.

To determine if Rac1 activation caused MIIA to specifically localize within FAs or to radial SFs [8, 27], we utilized TIRF microscopy and cell fractionation. Comparison of TIRF and Epi images of immunostained cells showed that in mock-transfected controls or cells expressing Rac1 N17, MIIA was associated with SFs on the ventral cell surface in the cell center and rear and SFs and arcs on the dorsal cortex [8] but was rarely in FAs and lamellipodia (Figures 1B and S2). In cells expressing Rac1V12, MIIA localized to dorsal arcs and dorsal and ventral SFs, similar to controls, but was additionally prominently colocalized with paxillin in FAs (Figures 1B and S2). Quantification showed that in controls or cells expressing Rac1N17, 46% of FAs contained some MIIA staining; expression of Rac1V12 increased this to 65% (Figure 1C). Similarly, in controls or cells expressing Rac1N17, the fraction of FA area that was co-occupied by MIIA and paxillin was relatively low (17%) but was significantly increased in cells expressing Rac1V12 (25%) (Figure 1D). To confirm our localization data, we separated the cell body fraction from the substrate-adhered FA fraction, with or without additional Rac1V12 expression, and performed western blot analysis. This showed that constitutive activation of Rac1 increased MIIA in the FA fraction 1.6-fold compared to control (Figure 1E). Thus, active Rac1 specifically enhances MIIA association with FAs.

Rac1 Activation Induces Capture and Assembly of MIIA Minifilaments in Maturing FAs

We next sought to determine how Rac1 activity affects the association of MIIA with FA in live cells. We performed

time-lapse TIRF microscopy of cells expressing MIIA HC fused via its N terminus (head domain) to GFP (GFP-MIIA), a fusion protein that complements MIIA null in mice [28]. This was coexpressed with mApple paxillin, with or without the additional expression of Rac1 mutants. In peripheral regions of the cell where MIIA density was low, GFP-MIIA was always present as dual diffraction-limited puncta whose peaks were separated by 300 ± 16 nm (Figure 2A). Immunostaining of cells expressing GFP-MIIA with antibodies that recognize an epitope in the C terminus of MIIA revealed that the rod was localized between the dual punctae of GFP-labeled heads (Figure 2A). Thus, dual punctae of GFP-MIIA represent individual bipolar MIIA minifilaments in which two bouquets of actin-binding heads are separated by a 300 nm bare zone of bundled MII rods [29–31].

Time-lapse movies (at 10 s intervals) showed that in control cells, GFP-MIIA minifilaments exhibited two distinct dynamic behaviors. In the predominant behavior, as the leading edge underwent protrusion/retraction dynamics, randomly oriented individual minifilaments appeared in the lamellipodium, underwent rapid retrograde flow for a few micrometers, and then oriented parallel to the leading edge concurrent with slowing of retrograde flow, without association with mApple paxillin-labeled FA (Figure 2C; Movies S1 and S2). The assembly, retrograde flow, and parallel orientation of many GFP-MIIA minifilaments contributed to formation of concave arcs that spanned between FA [7, 27]. In the second, less prevalent behavior, GFP-MIIA minifilaments appeared perpendicular to the leading edge in maturing FA near the base of the lamellipodium (Figure 2B; Movie S2). Quantification showed that minifilaments within FA were predominantly oriented parallel to the FA, whereas minifilaments outside of FA were not (Figure 2E). Thus, most GFP-MIIA minifilaments assemble in the lamellipodium to promote formation of contractile arcs, whereas a subset assembles in maturing FA, where they align along the FA long axis.

In cells expressing Rac1V12, GFP-MIIA also exhibited these two behaviors, but minifilament assembly within FAs was much more prevalent than in controls (Figure 2D; Movies S2 and S3). In addition, minifilaments undergoing retrograde flow in the lamellipodium were often captured by FA, where they either remained stationary or moved rearward in tandem with FA growth. Quantification demonstrated that like controls, in cells expressing Rac1V12 minifilaments in FAs were oriented along the FA axis (Figure 2E). In contrast, in cells expressing DN Rac1, GFP-MIIA did not associate with FAs (Figures 1A and 1B; Movie S4). Thus, Rac1 activation promotes the assembly and capture of MIIA minifilaments in maturing FA; however, minifilament orientation is driven by FA association rather than Rac1 activation per se.

Rac1 Activation Promotes Phosphorylation of MIIA HC on S1916 in FAs in an Integrin-Dependent Manner

To determine how adhesion and Rac1 activation regulate MIIA association with FA, we analyzed their effects on MIIA HC phosphorylation. Integrin engagement to fibronectin or collagen extracellular matrices (ECMs) induces Rac1 activation [11, 12], whereas fibronectin engagement promotes phosphorylation of MIIA HC on serine 1916 (pS1916 MIIA HC) [32]. We performed western blot analysis with pS1916 MIIA HC phosphospecific antibodies of lysates from cells with Rac1 activity manipulated that were plated on either fibronectin or collagen. This showed that on either ECM, Rac1V12 increased pS1916 MIIA HC over 2-fold compared to controls. However, expression of Rac1N17 did not reduce pS1916 MIIA below control levels, suggesting that Rac1-independent mechanisms promote pS1916 (Figures 3B and 3C). Plating cells on poly-L-lysine to inhibit integrin engagement showed that Rac1V12 expression did not increase pS1916 MIIA HC over Rac1N17 expression or controls, in spite of the fact that Rac1V12 activated downstream signaling, as evidenced by an increase in phosphorylation of one of its downstream targets, Pak1 (Figure 3A). Thus, Rac1 mediates pS1916 MIIA HC in an integrin-dependent, Pak1-independent manner.

To determine the relationship between Rac1-induced MIIA recruitment to FAs and pS1916 phosphorylation, cells were immunostained for pS1916 MIIA HC and paxillin followed by TIRF imaging. This showed that in controls, pS1916 MIIA HC localized to peripheral SFs and a small fraction of FA. Rac1V12 markedly increased colocalization of pS1916 MIIA HC with FA, whereas expression of Rac1N17 reduced pS1916 MIIA HC staining throughout the cell (Figure 3E). Because Rac1 activity and MIIA HC phosphorylation are thought to inhibit MII filament assembly in vitro and in cells [33, 34], we examined the effects of Rac1 activation on the triton solubility of MIIA. Although RacV12 promoted pS1916 MIIA HC (Figures 3B and 3C), it induced no major change in total MIIA solubility compared to controls or cells expressing Rac1N17. However, the fraction of MIIA that was phosphorylated became concentrated in the soluble fraction (Figure 3D). This agrees with the previous studies and further suggests that Rac1-mediated phosphorylation affects only a small fraction of total MIIA, and that the FA-associated fraction of pS1916 MIIA is locally protected against cytoskeletal dissociation. Thus, Rac1 activation promotes pS1916 MIIA HC in an integrin-dependent, Pak1-independent manner to promote specific association of pS1916 MIIA minifilaments with FAs.

Indicators of Rac1 Activation during Cell Spreading and ECM Stiffness Mechanosensing Correlate with pS1916 MIIA HC at FAs

To determine if the Rac1-dependent pathway of MIIA phosphoregulation occurs in response to physiological stimulation of Rac1 activity, we examined MIIA HC phosphorylation and localization during cell spreading [11] and ECM stiffness mechanosensing [35]. Cells were lysed in suspension or during spreading at 15, 30, 45, 60, and 90 min after plating on fibronectin and analyzed by western blotting. This showed that, compared to suspended cells, the level of pS1916 MIIA HC increased 3-fold and plateaued 45 min after plating (Figures 4A and 4B). Probing for phosphorylation of downstream targets of Rac1 (Pak1 and Lim kinase) and integrin signaling (FAK) showed that indicators of Rac1 activity increased and plateaued with kinetics similar to those of pS1916 IIA HC, whereas FAK activity peaked at 60 min and declined by 90 min (Figures 4A and 4B). TIRF images of cells expressing GFP-MIIA HC and mApple paxillin at specific times after plating on fibronectin showed that GFP-MIIA HC recruitment and localization to FA mirrored the kinetics of pS1916 MIIA HC seen by western blot (Figure 4C). Thus, activation of downstream targets of Rac1 during cell adhesion and spreading correlate with pS1916 MIIA HC and localization in FA.

Recent studies have shown that cellular mechanosensation in response to increased stiffnesses induces Rac activation [36]. To determine if Rac1 activation induced by ECM stiffness mechanosensing promotes S1916 MIIA phosphorylation and FA localization, we plated cells on fibronectin-coupled

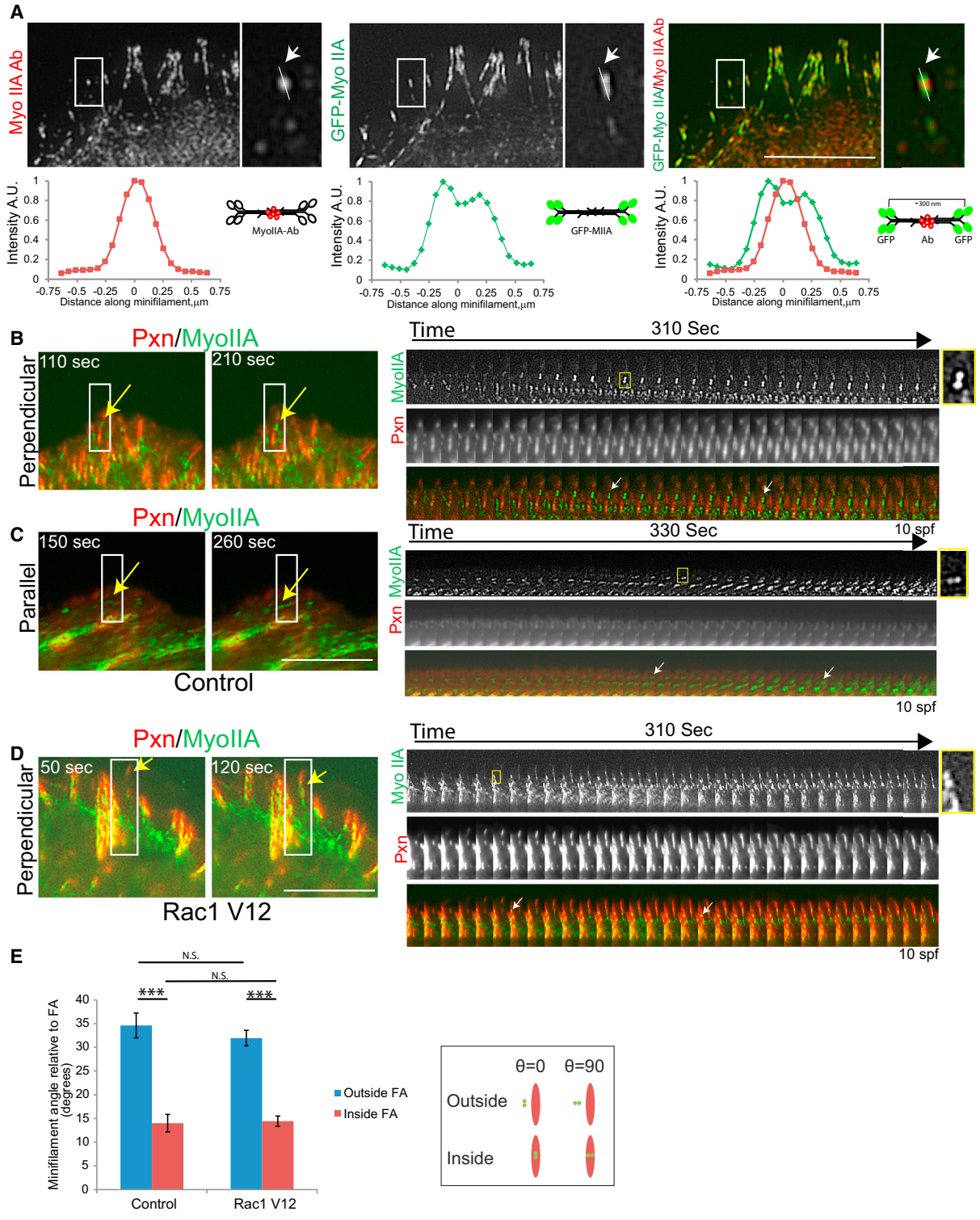

Figure 2. Rac1 Induces Capture, Assembly, and Orientation of MIIA Minifilaments in FAs

(A) U2OS cells expressing GFP-MIIA (green) immunostained with antibodies to the MIIA rod (myosin IIA Ab, red), TIRF images. Zooms, high magnification of boxed regions. Scale bar, 10 μm. Below, intensity along lines highlighted with arrow in zoomed panels; x axis, distance from the peak myosin IIA Ab intensity; cartoons, location of N-terminal GFP (green) or antibody binding site (red).

(B–D) Time-lapse TIRF of U2OS cells expressing GFP-MIIA (green) and mApple paxillin (red). Left: color overlay; scale bar, 10 μm. Right: time series (10 s intervals) of GFP-MIIA (upper) mApple paxillin (middle) and color overlays (bottom) of the boxed region. White arrows: single MIIA minifilaments at time points shown on left, yellow box: single minifilament zoomed at far right. (B) GFP-MIIA minifilament captured at growing FA. (C) GFP-MIIA minifilament undergoing retrograde flow. (D) GFP-MIIA in a cell expressing Rac1(V12). spf, sec per frame.

(E) Quantitation of the orientation of minifilaments located inside and outside FA. Control: n = 5 cells; Rac1V12: n = 4 cells; ~75 minifilaments/cell analyzed. Error bars = SEM; NS, $p > 0.05$; ***$p < 0001$.

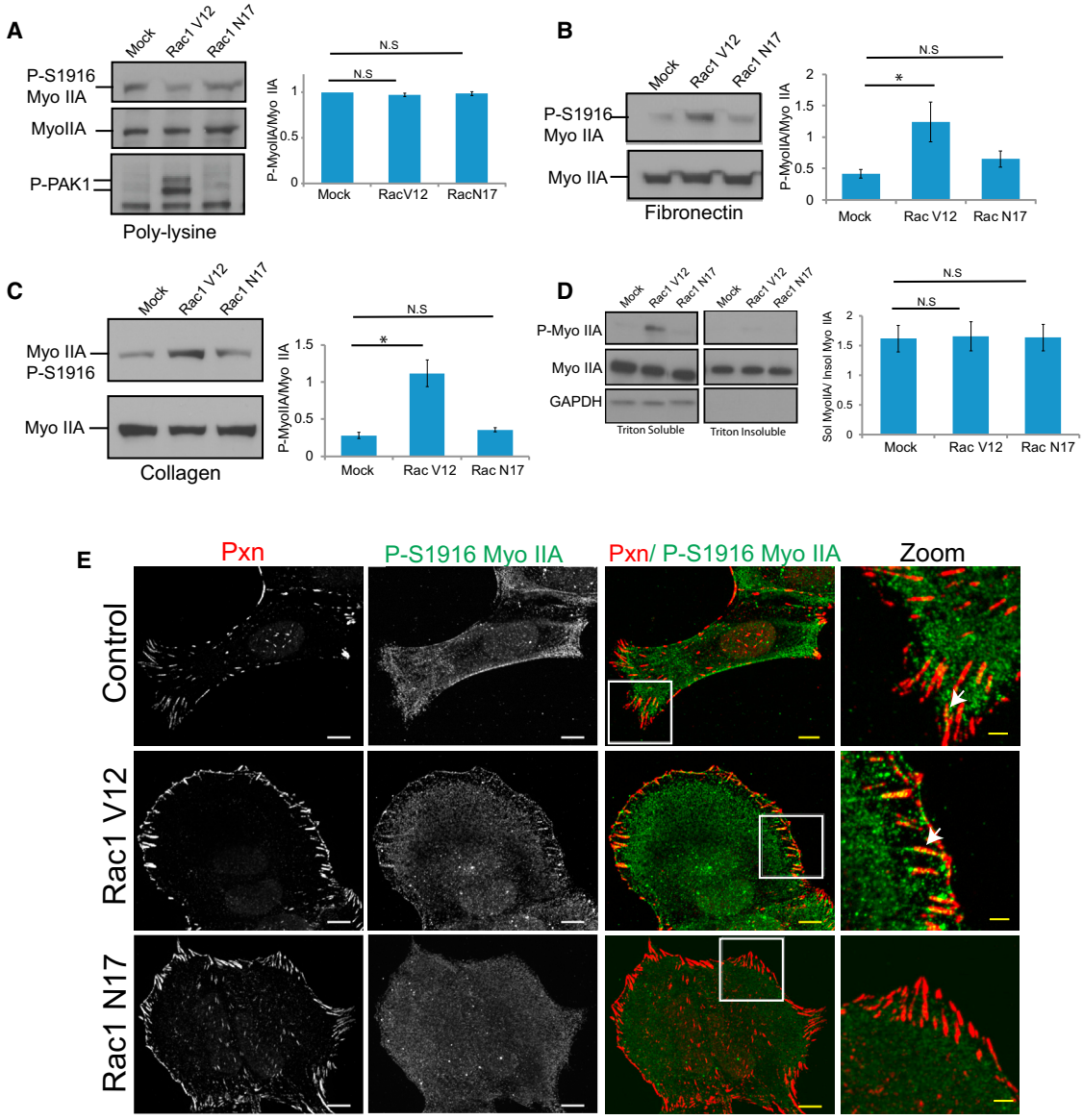

Figure 3. Rac1 Activation Promotes Phosphorylation of MIIA HC on S1916 in FAs in an Integrin-Dependent Manner

(A–C) U2OS cells cultured on poly-L-lysine (A), fibronectin (B), or collagen (C) and either mock transfected or transfected with Rac1V12 or Rac1N17 Rac1 mutants. Western blot with antibodies to MIIA (Myo IIA), Pak1 phosphorylated on serines 199 and 204 (P-Pak1), or MIIA phosphorylated on serine 1916 (P-S1916 Myo IIA).

(D) Triton X-100 extraction and centrifugal separation of triton-insoluble cytoskeleton pellet from triton soluble cytosolic supernatant. Western blot with antibodies to MIIA, P-S1916 Myo IIA, and glyceraldehyde 3-phosphate dehydrogenase (GAPDH).

In (A)–(D), quantification of western blots (right panels) (A, C, and D) n = 3, in (B), n = 5; error bars = SEM; NS, $p > 0.05$; *$p < 0.05$.

(E) TIRF images of U2OS cells either mock transfected (control) or transfected with Rac1V12 or Rac1N17 Rac1 mutants and immunostained for paxillin (red, Pxn) and P-S1916 MIIA (green). Zoom: high magnification of boxed regions; bars = 10 μm in lower-magnification images, 3 μm in zooms; white arrow, P-S1916 MyoIIA localization at FA.

polyacrylamide gels of defined stiffness (0.7, 8.6, 55 kPa; Figures 4D and 4E). Western blot showed that pS1916 MIIA HC was higher in cells adhered to intermediate stiffness ECM compared to either lower (0.7 kPa) or higher (55 kPa) stiffness ECMs (Figure 4E). Confocal imaging of cells expressing GFP-MIIA HC and mApple paxillin on compliant ECMs showed that GFP-MIIA FA recruitment was highest in cells adhered to intermediate stiffness ECMs (Figure 4D). Time-lapse phase-contrast imaging of cells plated on different stiffness ECMs showed that cells migrated the fastest on intermediate stiffness (Figure 4F). These results show that, similar to downstream indicators of Rac1 activation, pS1916 MIIA HC and localization to FA is induced by cell spreading and ECM stiffness mechanosensing, suggesting that these stimuli induce Rac1-mediated phosphoregulation of MIIA HC.

PKC Activity Is Necessary and Sufficient for Rac1-Dependent pS1916 MIIA HC at FA

Rac1 and PKCs are activated by integrin engagement [10, 11, 25], and PKCs can phosphorylate S1916 of MIIA HC [21]. We used pharmacological manipulation of PKC activity to determine the involvement of PKC in the Rac1- and

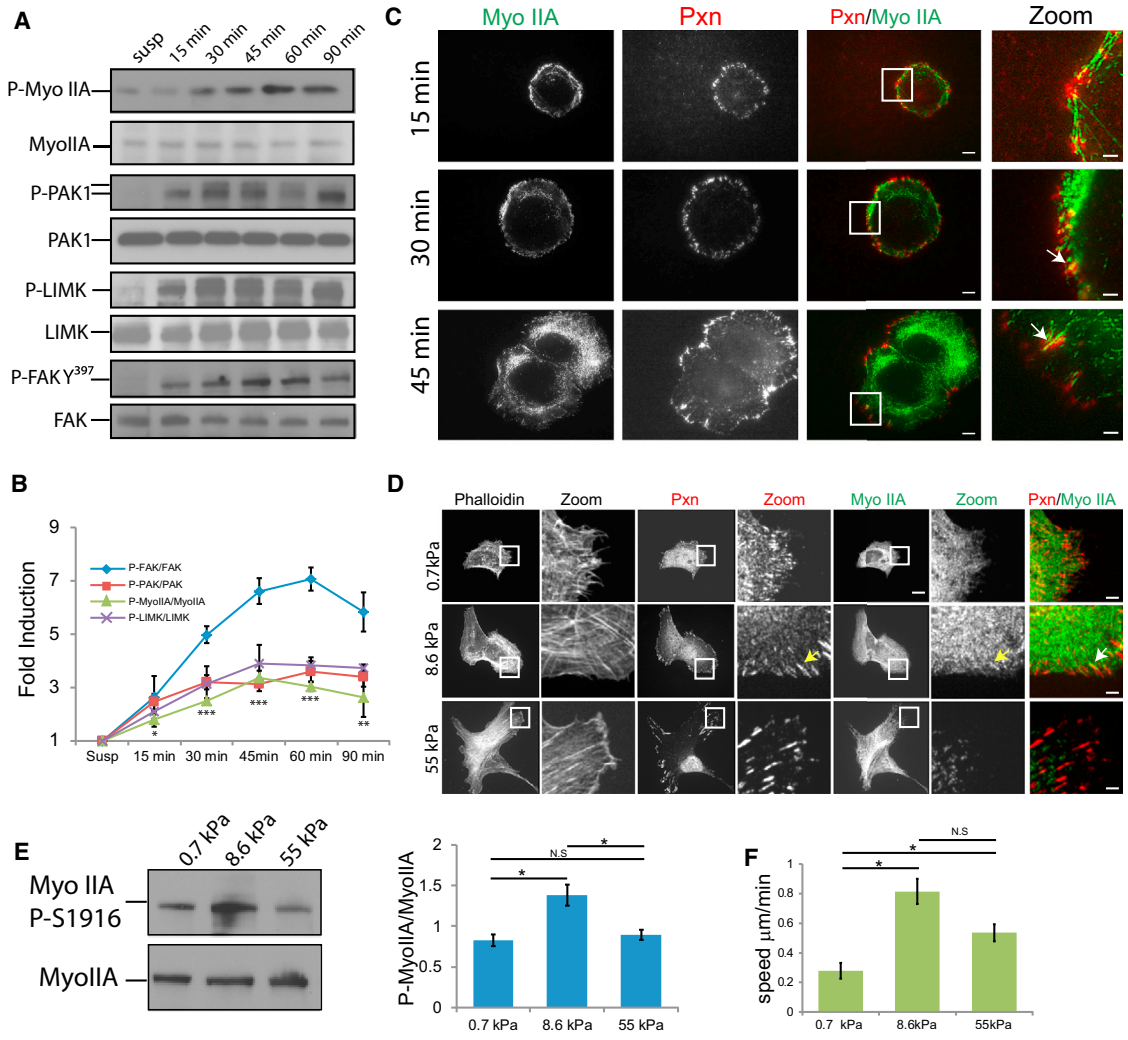

Figure 4. Downstream Target Proteins of Rac1 Activation during Cell Spreading and ECM Stiffness Mechanosensing Correlate with Phosphorylation of MIIA S1916 at FA

(A and B) U2OS cells spreading on fibronectin harvested at the time noted after plating, western blot with antibodies to MIIA (Myo IIA), MIIA phosphorylated on serine 1916 (P-Myo IIA), Pak1, Pak1 phosphorylated on serines 199 and 204 (P-Pak1), Lim kinase (LIMK), Lim kinase phosphorylated on threonine 508 (P-LIMK), FAK, or FAK phosphorylated on tyrosine 397 (P-FAK Y^{397}). (B) Quantitation of three replicates of the experiment in (A), fold induction over suspension, n = 3.

(C) TIRF images of U2OS cells expressing GFP-MIIA (green) and mApple paxillin (red) spreading on fibronectin. In (C) and (D), zoom: higher magnification of boxed regions; arrows: pS1916 MIIA in FA; bars: 10 μm in lower-magnification images and 3 μm in zooms.

(D and E) Cells on fibronectin-coupled polyacrylamide substrates (stiffness noted).

(D) Confocal images of immunolocalized MIIA (green) and paxillin (red) and actin stained with fluorescent phalloidin.

(E) Western blot left, quantitation, right, n = 3 experiments.

(F) Migration velocity of cells on fibronectin-coupled substrates of noted stiffness. n = 10 cells/condition. Error bars = SEM; NS, $p > 0.05$; *$p < 0.05$; **$p < 0.01$; ***$p < 0.001$.

integrin-mediated regulation of MIIA HC. Treatment of mock-transfected controls or cells expressing Rac1 V12 with either the pan-PKC inhibitor Go6976 or the PKC βII-specific inhibitor CGP53353 blocked pS1916 MIIA HC and localization of MIIA to FAs in cells expressing Rac1 V12 but did not block Pak1 activation induced by Rac1 V12 or baseline pS1916 MIIA in control or RacN17-transfected cells (Figures 5A and 5B). In contrast, compared to cells expressing Rac1 N17 alone, treatment of cells expressing Rac1 N17 with phorbol-12-myristate-13-acetate (PMA) to activate PKCs increased pS1916 MIIA HC and induced localization of MIIA to FAs (Figures 5A and 5B). Thus, PKC activity is necessary and sufficient for Rac1-dependent induction of pS1916 MIIA HC and recruitment to FAs and specifically implicates PKCβII in this process.

pS1916 MIIA HC Is Necessary and Sufficient for Enhancing Its Assembly at FAs

Rac1 and PKC have multiple targets in addition to MIIA HC [37]. To determine the specific role of S1916 phosphorylation in MIIA function, we generated nonphosphorylatable (GFP-S1916A MIIA HC) and phosphomimic (GFP-S1916D MIIA HC) mutants of GFP-MIIA HC (wild-type [WT]). Experiments were performed in cells depleted of MIIA small interfering RNA (siRNA) (~90% knockdown after 72 hr, no effect on MIIB,

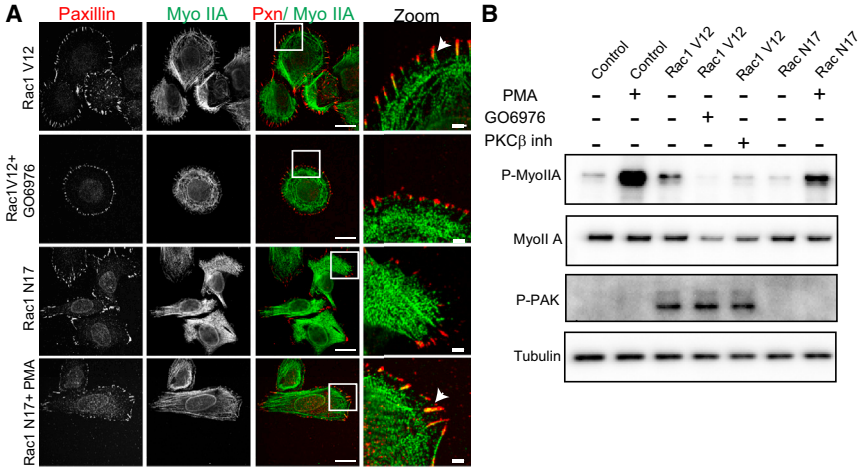

Figure 5. PKC Activity Is Necessary and Sufficient for Rac1-Dependent Induction of Phosphorylation of MIIA HC at FA

U2OS cells mock transfected (Control) or transfected with Rac1V12 or Rac1N17 Rac1 mutants were treated with GO6976 (pan-PKC inhibitor), CGP53353 (PKCβII inhibitor), or phorbol myristate acetate (PMA, PKC activator).

(A) TIRF images of immunofluorescence localization of MIIA (green) and paxillin (red). Zoom, higher magnification of boxed regions. Scale bars, 10 μm in lower-magnification images, 3 μm in zooms.

(B) Western blot with antibodies to antibodies to MIIA phosphorylated on serine 1916 (P-Myo IIA), PAK on serines 199 and 204 (P-PAK), MIIA (MyoIIA), or tubulin.

Figure 6A). MIIA HC knockdown produced long cell tails, randomly directed lamellipodia, and loss of mature FAs (Figure S3), similar to effects of blebbistatin [38]. Expression of WT GFP-MIIA HC in cells depleted of MIIA rescued these effects (Figure 3).

We then examined the effect of phosphomutants on MIIA localization and dynamics. GFP-tagged MIIA HC mutants were coexpressed with mApple paxillin in MIIA-knockdown cells at ~80% of the level of endogenous MIIA (Figure 6A). TIRF imaging and quantification showed that the fraction of FA area that was occupied by MIIA and the fraction of FA containing MIIAs was significantly higher in cells expressing GFP-S1916D MIIA HC than in cells expressing GFP MIIA HC or GFP-S1916A MIIA HC (Figures 6B, 6G, and 6H; Movie S5). Furthermore, coexpression of Rac1 V12 with GFP-S1916A MIIA HC did not enhance its localization to FAs compared to expression of GFP-S1916A MIIA HC alone, and GFP-S1916D MIIA HC localized to the FAs even in the presence of Rac1N17 (Figure 6B). These results suggest that S1916 phosphorylation is necessary and sufficient for MIIA association with FA.

We next determined how pS1916 MIIA HC associates with FA in live cells by TIRF microscopy of cells depleted of endogenous MIIA and coexpressing GFP-tagged MIIA HC mutants and mApple-paxillin. This showed that like WT GFP-MIIA HC, both phosphomutants formed bipolar minifilaments as evidenced by dual diffraction-limited punctae. For all three GFP-MIIA HC variants, most minifilaments appeared and assembled into arcs and did not colocalize with FAs (Figures 6C and 6D; Movie S5). However, in the presence or absence of Rac1N17, a substantial subset of GFP-S1916D MIIA HC minifilaments were captured and oriented or underwent de novo assembly at maturing FAs (Figures 6D and 6F; Movies S5 and S6), similar to the behavior of GFP-MIIA in cells expressing Rac1V12 (Figure 2D). This behavior was rare in cells expressing GFP-S1916A MIIA HC, even in the presence of Rac1V12 (Figure 6D; Movies S5 and S6). Together, these results suggest that S1916 phosphorylation is necessary and sufficient for MIIA assembly and capture at FAs.

pS1916 MIIA HC Promotes FA Assembly, Cell Migration, and Modulates ECM Stiffness Mechanosensing

We next sought to determine the effects of pS1916 MIIA on FA dynamics and cell behavior. We analyzed FA morphometry and dynamics in TIRF movies of cells depleted of endogenous MIIA and coexpressing GFP-tagged MIIA HC mutants and mApple-paxillin. This showed that depletion of MIIA reduced FA size, whereas GFP-S1916D MIIA HC or GFP-S1916A MIIA HC had no effect FA size compared to WT-GFP-MIIA HC (Figure 7A). However, GFP-S1916D MIIA HC increased FA number and density compared to WT GFP-MIIA HC, whereas GFP-S1916A-MIIA HC had no effect (Figures 7B and 7C). Movies (Movie S7) or time projections of mApple-paxillin-labeled FAs (Figure 7D) suggested that GFP-S1916D MIIA HC promoted FA turnover compared to WT GFP-MIIA HC, whereas GFP-S1916A MIIA HC appeared to reduce FA dynamics. Image autocorrelation analysis of FA in TIRF movies as a general measure of FA stability [39] supported this notion, demonstrating that GFP-S1916D MIIA HC reduced the half-time of image correlation decay relative to that of WT or GFP-S1916A MIIA HC (Figure 7E). Analysis of individual FA assembly/disassembly rates showed that compared to WT GFP-MIIA HC, GFP-S1916D MIIA HC increased FA assembly rate but did not affect FA disassembly rate, whereas GFP-S1916A MIIA HC did not affect FA assembly rate but slowed FA disassembly (Figures 7F and 7G). Time-lapse phase-contrast imaging of cells migrating on fibronectin-coated coverslips showed that GFP-S1916D MIIA HC increased, whereas GFP-S1916A MIIA HC decreased cell migration velocity compared to WTGFP-IIA HC (Figure 7H), similar to effects of these mutants on FA dynamics. Together, these results suggest that MIIA phosphorylation and/or recruitment to FAs promotes dynamic FA turnover and enhances cell migration.

Finally, we determined the role of S1916 MIIA HC in ECM stiffness mechanosensing. We assayed the ability of cells depleted of endogenous MIIA HC and re-expressing GFP-MIIA HC mutants to modulate traction force, spread area, and migration speed in response to different stiffnesses of fibronectin-coupled polyacrylamide substrates. High-resolution traction force microscopy (TFM) on cells depleted of endogenous MIIA HC and coexpressing GFP-tagged MIIA HC mutants and mApple-paxillin was used to assess total traction force per cell and spread cell area (Figures 7I and 7J). This showed that in cells expressing WT-GFP-MIIA HC or GFP-S1916A MIIA HC, traction force and cell area doubled in response to doubling ECM stiffness from 4.1 to 8.6 kPa, and force increased ~6-fold and cells spread significantly further when stiffness was further raised ~6-fold from 8.6 to 55 kPa. In contrast, cells expressing GFP-S1916D MIIA HC failed to

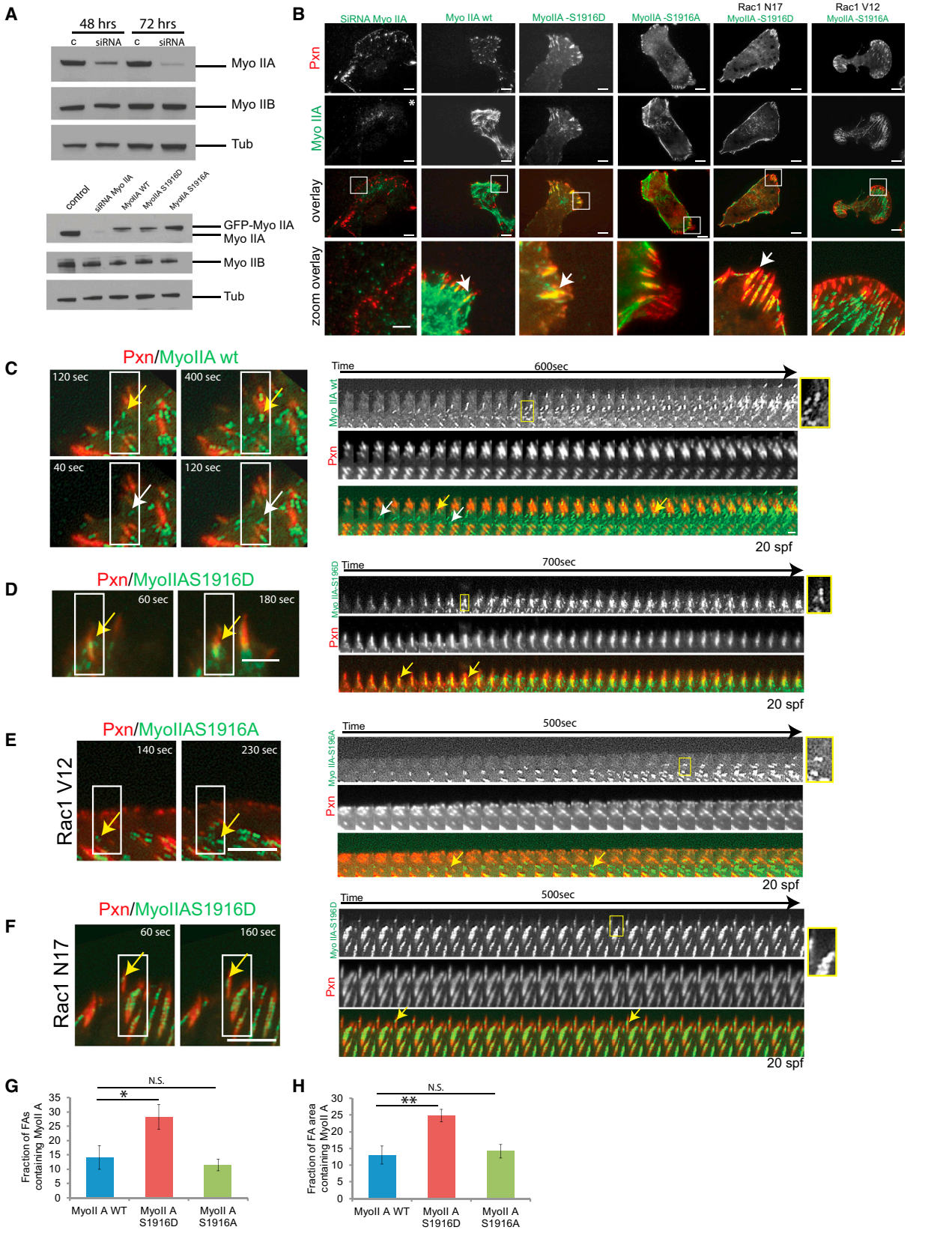

Figure 6. Phosphomimic Mutation S1916D Promotes MIIA HC Assembly at FA

U2OS cells treated with scrambled siRNAs (c) or siRNAs specific to the 3′ untranslated region of MIIA (siRNA MyoIIA) for the times noted, or additionally expressing GFP-MIIA (wild-type: MyoIIA WT) or GFP- MIIA bearing phosphomimic or nonphosphorylatable mutations in serine 1916 (phosphomimic: MyoIIA S1916D or nonphosphorylatable: MyoIIA S1916A).

(legend continued on next page)

increase traction force or spread area in response to shifting substrate stiffness from 4.1 to 8.6 kPa but were still responsive to the shift from 8.6 to 55 kPa, increasing both total traction force and cell area. Analysis of cell velocity showed that cells expressing WT GFP MIIA HC migrated faster on 8.6 kPa compared to on stiffer 55 kPa ECMs (Figure 7K), similar to the behavior of untransfected cells (Figure 4F). In contrast, although cells expressing either GFP-S1916A MIIA HC or GFP-S1916D MIIA HC exhibited faster and slower migration than wild-type GFP-MIIA HC, respectively, neither mutant showed differences in migration speed between soft and stiff ECMs. Thus, phosphoregulation of S1916 on MIIA HC is a critical modulator of cellular traction stress, migration speed, and cellular response to ECM stiffness.

Discussion

Our study reveals that Rac1 and integrin signaling induce PKC-mediated S1916 MIIA HC phosphorylation and shows for the first time that this signaling pathway promotes MIIA specific association with FAs and acts as a critical regulator of cellular traction stress, migration, and mechanosensation. We found that active Rac1 enhanced the association of MIIA, but not MIIB with FAs. PKC activity was necessary and sufficient for integrin- and Rac1-dependent phosphorylation of MIIA HC on S1916 and recruitment into FA, and may be mediated by the calcium-activated PKCβII. We demonstrated that Rac1-dependent S1916 phosphorylation and FA localization of MIIA HC occurs during cell spreading and ECM stiffness mechanosensing. Experiments with phosphomimic and nonphosphorylatable mutants of MIIA HC demonstrated that S1916 phosphorylation was necessary and sufficient for enhancing the capture and assembly of MIIA minifilaments at FA, and that phosphoregulation at this site promotes FA turnover to enhance cell migration and modulates the range ECM stiffnesses to which cells respond by changing their traction force, spreading, and migration speed.

The discovery of specific recruitment of MIIA to FA is surprising, because MII has not been considered as a bona fide FA protein. In spite of the fact that it has been identified in FA proteomes [40–42], it is generally thought that MII regulates FA maturation and turnover by promoting actin bundling or transmitting force through the actin network to FAs from a distance [4, 9]. Furthermore, recent evidence suggests that high traction forces at FA are generated by acto-myosin arcs, not by radial SFs that are attached to FAs [43]. Our data support this notion, because we found that S1916 MIIA HC phosphomimic that promotes MIIA recruitment to radial SF and FA decreased traction force. However, whether individual FA containing this mutant had altered force or if this was due to effects on global MII assembly/disassembly was not determined.

So what is MIIA doing in FA? We suggest that myosin IIA could be directly promoting assembly and maturation at the single FA level by locally driving integrin clustering and/or activation by applying localized force to the ECM bound integrin-linked actin filaments [44, 45]. Alternatively, MIIA minifilaments within FA could mediate recently observed traction force fluctuations in single FAs that are required for ECM stiffness mechanosensing and durotaxis [46]. In support of this, both traction force fluctuations and MIIA recruitment only occur in a subset of FA, and force fluctuations are not synchronized between neighboring FA in the same cell [46], implying that fluctuations are produced by very local contraction. Whether Rac1 activation or MIIA HC phosphorylation regulates force fluctuations in single FAs or is required for durotaxis remains to be determined.

Our results showing that phosphorylation of MIIA HC promotes assembly of minifilaments specifically within FAs contradicts the notion that phosphorylation of MIIA HC promotes minifilament disassembly both in vitro and in cells [33, 47]. How phosphorylation at S1916 targets MIIA to FA and how this location protects phosphorylated minifilaments from disassembly we do not know. However, the calcium-activated PKCβII, as well as Rac1, have been identified as members of the FA proteome [41]. Thus, it is possible that local phosphorylation of MIIA within FAs and/or binding of pS1916 by an FA protein modulate the effect of phosphorylation on minifilament assembly dynamics at the single FA level.

Our findings support previous studies that integrins [32], Rac1 [23], and PKC [33] are critical physiological regulators of MII HC phosphorylation. However, these regulators have not previously been linked in a pathway for site-specific phosphorylation of the IIA isoform or its association with FAs. Previous reports showed that fibronectin and collagen both induce Rac1 activation [11, 12], whereas fibronectin, but not collagen, induces PKCα activation [25, 48]. However, our findings suggest a novel pathway in which Rac1 and collagen or fibronectin-mediated activation of PKCβII promotes MIIA phosphorylation. Furthermore, whereas previous studies implicate Pak in mediating MII HC phosphorylation at unknown sites [23, 49], our results suggest Rac1-mediated phosphorylation of MIIA HC S1916 is independent of Pak. It is possible that this novel pathway mediates the upregulation of S1916 MIIA HC phosphorylation in epithelial-to-mesenchymal transition [50], mast cell degranulation [51], and tumor cell migration [32], all of which have been linked to Rac1 activity [52–54].

Supplemental Information

Supplemental Information includes Supplemental Experimental Procedures, three figures, and seven movies and can be found with this article online at http://dx.doi.org/10.1016/j.cub.2014.11.043.

Acknowledgments

We thank Bill Shin for maintaining C.M.W.'s lab microscopes, Schwanna Thacker for administrative assistance, and Jordan Beach and the Sellers and Adelstein labs at NHLBI for helpful discussions. A.M.P., L.B.C.,

(A) Western blot with antibodies to MIIA, MIIB, or tubulin.
(B) TIRF images of immunolocalized paxillin (red). The cell in the first column second row was additionally processed for immunolocalization of MIIA (asterisk). Zoom, higher magnification of boxed regions; arrows, FA. Scale bars, 10 μm in lower-magnification images, 3 μm in zooms.
(C–F) TIRF movies of U2OS cells depleted of endogenous MIIA by siRNA and expressing GFP-MIIA mutants (green) and mApple paxillin (red) with (E and F) or without (C and D) additional expression of Rac1V12 (E) or Rac1N17 (F) Rac1 mutants. Left: color overlays at the times noted by arrows on right. Scale bar, 2 μm. Right: time series (20 s intervals) of GFP-MIIA, mApple paxillin, and color overlays of the boxed regions at left; yellow box, single minifilament zoom at far right. White arrows in (C): minifilament undergoing retrograde flow; yellow arrows, minifilament colocalized with a FA.
(G and H) Fraction of FAs that contain MIIA staining: (G) fraction of FA area per cell co-occupied by MIIA (H) from TIRF images. Myo IIA WT: n = 7 cells; Myo IIA S1916D: n = 11 cells; Myo IIA S1916A: n = 8 cells; ~50 FA/cell. Error bars = SEM; NS, $p > 0.05$; *$p < 0.05$; **$p < 0.01$.

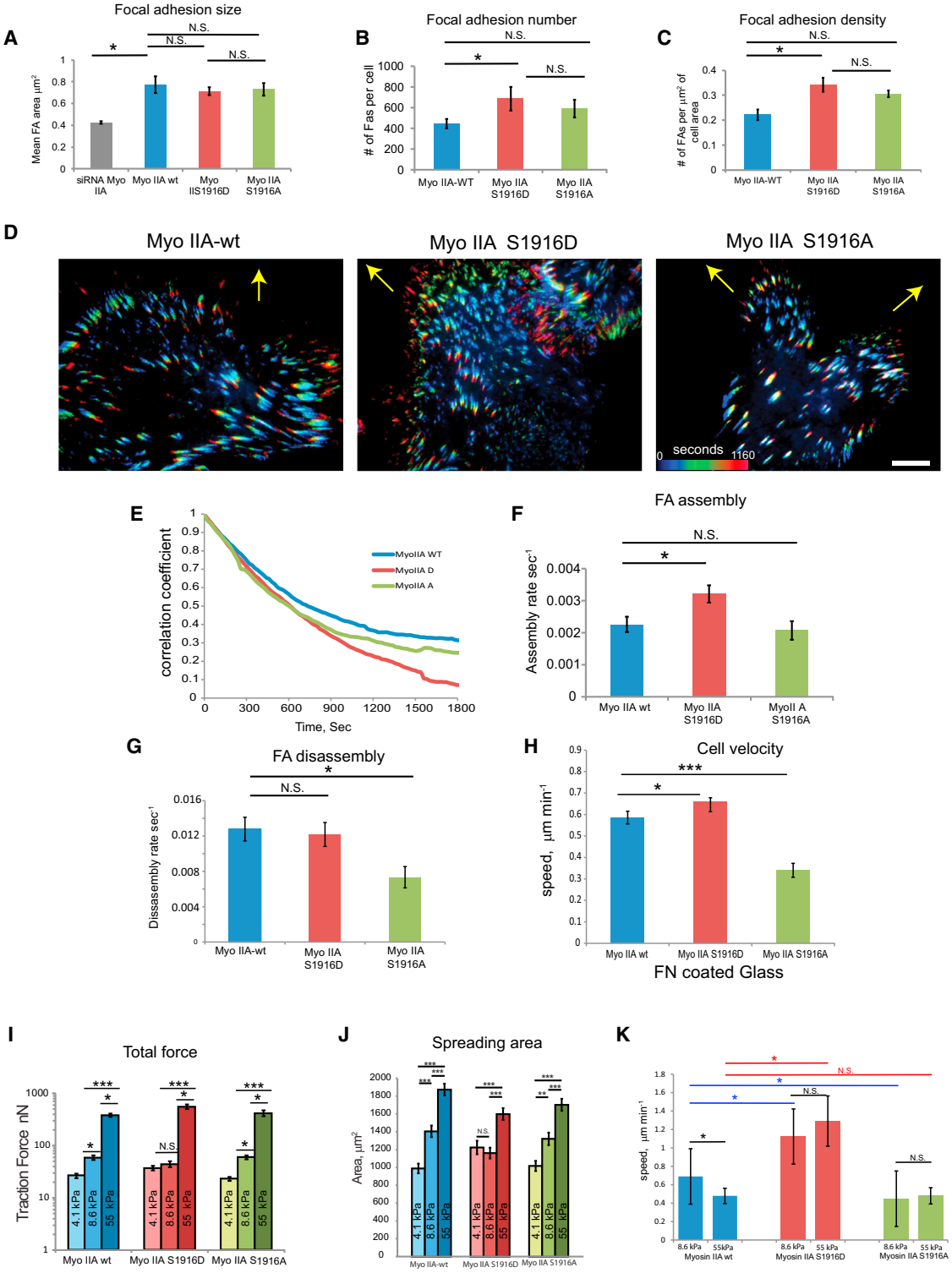

Figure 7. Phosphoregulation of MIIA HC on S1916 Promotes FA Assembly, Enhances Cell Migration, and Modulates ECM Stiffness Mechanosensing

U2OS cells depleted of endogenous MIIA by siRNA and expressing mApple paxillin with or without (siRNA MyoIIA) additional the expression of GFP-MIIA variants (wild-type: MIIA WT, phosphomimic: MIIA S1916D, nonphosphorylatable: MIIA S1916A).

(A–C) FA size (A), number per cell (B), and density (C) from TIRF images (siRNA Myo IIA: n = 648 FAs, six cells; WT: n = 3,549 FAs, eight cells; S1916D: n = 5,713 FAs, eight cells; S1916A: n = 4,118 FAs, seven cells).

(D) Color-coded maximal-intensity projection time-montages of time-lapse TIRF image series of mApple paxillin. Yellow arrow, direction of cell protrusion. Scale bar, 10 µm.

(E) Image autocorrelation analyses of TIRF series.

(F and G) Mean FA assembly (F) and disassembly (G) rates (WT: n = 1,301, eight cells; S1916D: n = 3,248 FAs, eight cells; S1916A: n = 2,109 FAs, seven cells).

(H) Cell migration velocity on fibronectin-coupled glass coverslips from phase-contrast movies.

(legend continued on next page)

S.V.P., R.S.F., and C.M.W. were supported by the NHLBI Division of Intramural Research. T.T.E. was supported by NIH grant GM50009.

Received: February 19, 2014
Revised: July 14, 2014
Accepted: November 14, 2014
Published: December 24, 2014

References

1. Vicente-Manzanares, M. (2013). Cell migration: cooperation between myosin II isoforms in durotaxis. Curr. Biol. *23*, R28–R29.
2. Conti, M.A., and Adelstein, R.S. (2008). Nonmuscle myosin II moves in new directions. J. Cell Sci. *121*, 11–18.
3. Kolega, J. (2003). Asymmetric distribution of myosin IIB in migrating endothelial cells is regulated by a rho-dependent kinase and contributes to tail retraction. Mol. Biol. Cell *14*, 4745–4757.
4. Vicente-Manzanares, M., Zareno, J., Whitmore, L., Choi, C.K., and Horwitz, A.F. (2007). Regulation of protrusion, adhesion dynamics, and polarity by myosins IIA and IIB in migrating cells. J. Cell Biol. *176*, 573–580.
5. Verkhovsky, A.B., Svitkina, T.M., and Borisy, G.G. (1995). Myosin II filament assemblies in the active lamella of fibroblasts: their morphogenesis and role in the formation of actin filament bundles. J. Cell Biol. *131*, 989–1002.
6. Vicente-Manzanares, M., Newell-Litwa, K., Bachir, A.I., Whitmore, L.A., and Horwitz, A.R. (2011). Myosin IIA/IIB restrict adhesive and protrusive signaling to generate front-back polarity in migrating cells. J. Cell Biol. *193*, 381–396.
7. Burnette, D.T., Manley, S., Sengupta, P., Sougrat, R., Davidson, M.W., Kachar, B., and Lippincott-Schwartz, J. (2011). A role for actin arcs in the leading-edge advance of migrating cells. Nat. Cell Biol. *13*, 371–381.
8. Hotulainen, P., and Lappalainen, P. (2006). Stress fibers are generated by two distinct actin assembly mechanisms in motile cells. J. Cell Biol. *173*, 383–394.
9. Choi, C.K., Vicente-Manzanares, M., Zareno, J., Whitmore, L.A., Mogilner, A., and Horwitz, A.R. (2008). Actin and alpha-actinin orchestrate the assembly and maturation of nascent adhesions in a myosin II motor-independent manner. Nat. Cell Biol. *10*, 1039–1050.
10. Ridley, A.J. (2011). Life at the leading edge. Cell *145*, 1012–1022.
11. Price, L.S., Leng, J., Schwartz, M.A., and Bokoch, G.M. (1998). Activation of Rac and Cdc42 by integrins mediates cell spreading. Mol. Biol. Cell *9*, 1863–1871.
12. Suzuki-Inoue, K., Yatomi, Y., Asazuma, N., Kainoh, M., Tanaka, T., Satoh, K., and Ozaki, Y. (2001). Rac, a small guanosine triphosphate-binding protein, and p21-activated kinase are activated during platelet spreading on collagen-coated surfaces: roles of integrin alpha(2) beta(1). Blood *98*, 3708–3716.
13. Wittmann, T., Bokoch, G.M., and Waterman-Storer, C.M. (2003). Regulation of leading edge microtubule and actin dynamics downstream of Rac1. J. Cell Biol. *161*, 845–851.
14. Nobes, C.D., and Hall, A. (1995). Rho, rac, and cdc42 GTPases regulate the assembly of multimolecular focal complexes associated with actin stress fibers, lamellipodia, and filopodia. Cell *81*, 53–62.
15. Giannone, G., Dubin-Thaler, B.J., Rossier, O., Cai, Y., Chaga, O., Jiang, G., Beaver, W., Döbereiner, H.G., Freund, Y., Borisy, G., and Sheetz, M.P. (2007). Lamellipodial actin mechanically links myosin activity with adhesion-site formation. Cell *128*, 561–575.
16. Adelstein, R.S., Pato, M.D., Sellers, J.R., de Lanerolle, P., and Conti, M.A. (1982). Regulation of contractile proteins by reversible phosphorylation of myosin and myosin kinase. Soc. Gen. Physiol. Ser. *37*, 273–281.
17. Vicente-Manzanares, M., Ma, X., Adelstein, R.S., and Horwitz, A.R. (2009). Non-muscle myosin II takes centre stage in cell adhesion and migration. Nat. Rev. Mol. Cell Biol. *10*, 778–790.
18. Goeckeler, Z.M., Masaracchia, R.A., Zeng, Q., Chew, T.L., Gallagher, P., and Wysolmerski, R.B. (2000). Phosphorylation of myosin light chain kinase by p21-activated kinase PAK2. J. Biol. Chem. *275*, 18366–18374.
19. Zeng, Q., Lagunoff, D., Masaracchia, R., Goeckeler, Z., Côté, G., and Wysolmerski, R. (2000). Endothelial cell retraction is induced by PAK2 monophosphorylation of myosin II. J. Cell Sci. *113*, 471–482.
20. Zhang, H., Webb, D.J., Asmussen, H., Niu, S., and Horwitz, A.F. (2005). A GIT1/PIX/Rac/PAK signaling module regulates spine morphogenesis and synapse formation through MLC. J. Neurosci. *25*, 3379–3388.
21. Dulyaninova, N.G., and Bresnick, A.R. (2013). The heavy chain has its day: regulation of myosin-II assembly. BioArchitecture *3*, 77–85.
22. Even-Faitelson, L., Rosenberg, M., and Ravid, S. (2005). PAK1 regulates myosin II-B phosphorylation, filament assembly, localization and cell chemotaxis. Cell. Signal. *17*, 1137–1148.
23. van Leeuwen, F.N., van Delft, S., Kain, H.E., van der Kammen, R.A., and Collard, J.G. (1999). Rac regulates phosphorylation of the myosin-II heavy chain, actinomyosin disassembly and cell spreading. Nat. Cell Biol. *1*, 242–248.
24. Slater, S.J., Seiz, J.L., Stagliano, B.A., and Stubbs, C.D. (2001). Interaction of protein kinase C isozymes with Rho GTPases. Biochemistry *40*, 4437–4445.
25. Mostafavi-Pour, Z., Askari, J.A., Parkinson, S.J., Parker, P.J., Ng, T.T., and Humphries, M.J. (2003). Integrin-specific signaling pathways controlling focal adhesion formation and cell migration. J. Cell Biol. *161*, 155–167.
26. Webb, D.J., Zhang, H., and Horwitz, A.F. (2005). Cell migration: an overview. Methods Mol. Biol. *294*, 3–11.
27. Burnette, D.T., Shao, L., Ott, C., Pasapera, A.M., Fischer, R.S., Baird, M.A., Der Loughian, C., Delanoe-Ayari, H., Paszek, M.J., Davidson, M.W., et al. (2014). A contractile and counterbalancing adhesion system controls the 3D shape of crawling cells. J. Cell Biol. *205*, 83–96.
28. Zhang, Y., Conti, M.A., Malide, D., Dong, F., Wang, A., Shmist, Y.A., Liu, C., Zerfas, P., Daniels, M.P., Chan, C.C., et al. (2012). Mouse models of MYH9-related disease: mutations in nonmuscle myosin II-A. Blood *119*, 238–250.
29. Billington, N., Wang, A., Mao, J., Adelstein, R.S., and Sellers, J.R. (2013). Characterization of three full-length human nonmuscle myosin II paralogs. J. Biol. Chem. *288*, 33398–33410.
30. Ebrahim, S., Fujita, T., Millis, B.A., Kozin, E., Ma, X., Kawamoto, S., Baird, M.A., Davidson, M., Yonemura, S., Hisa, Y., et al. (2013). NMII forms a contractile transcellular sarcomeric network to regulate apical cell junctions and tissue geometry. Curr. Biol. *23*, 731–736.
31. Niederman, R., and Pollard, T.D. (1975). Human platelet myosin. II. In vitro assembly and structure of myosin filaments. J. Cell Biol. *67*, 72–92.
32. Betapudi, V., Gokulrangan, G., Chance, M.R., and Egelhoff, T.T. (2011). A proteomic study of myosin II motor proteins during tumor cell migration. J. Mol. Biol. *407*, 673–686.
33. Dulyaninova, N.G., Malashkevich, V.N., Almo, S.C., and Bresnick, A.R. (2005). Regulation of myosin-IIA assembly and Mts1 binding by heavy chain phosphorylation. Biochemistry *44*, 6867–6876.
34. Murakami, N., Singh, S.S., Chauhan, V.P., and Elzinga, M. (1995). Phospholipid binding, phosphorylation by protein kinase C, and filament assembly of the COOH terminal heavy chain fragments of nonmuscle myosin II isoforms MIIA and MIIB. Biochemistry *34*, 16046–16055.
35. Clark, K., Langeslag, M., Figdor, C.G., and van Leeuwen, F.N. (2007). Myosin II and mechanotransduction: a balancing act. Trends Cell Biol. *17*, 178–186.
36. Bae, Y.H., Mui, K.L., Hsu, B.Y., Liu, S.L., Cretu, A., Razinia, Z., Xu, T., Puré, E., and Assoian, R.K. (2014). A FAK-Cas-Rac-lamellipodin signaling module transduces extracellular matrix stiffness into mechanosensitive cell cycling. Sci. Signal. *7*, ra57.
37. DeMali, K.A., Wennerberg, K., and Burridge, K. (2003). Integrin signaling to the actin cytoskeleton. Curr. Opin. Cell Biol. *15*, 572–582.
38. Aratyn-Schaus, Y., Oakes, P.W., and Gardel, M.L. (2011). Dynamic and structural signatures of lamellar actomyosin force generation. Mol. Biol. Cell *22*, 1330–1339.

(I–K) Quantitation of total traction force (I, WT: 4.1 kPa, eight cells; 8.6 kPa, six cells; 55 kPa, ten cells; 1916D: 4.1 kPa, five cells; 8.6 kPa, five cells; 55 kPa, ten cells; 1916A: 4.1 kPa, eight cells; 8.6 kPa, eight cells; 55 kPa, eight cells), spread area (J, > 60 cells analyzed per condition), and migration velocity (K) for cells on fibronectin-coupled substrates of the noted stiffness. Error bars in (A)–(C) and (G)–(K) = SEM; NS, $p > 0.05$; *$p < 0.05$; **$p < 0.01$; ***$p < 0.001$.

39. Zaidel-Bar, R., Milo, R., Kam, Z., and Geiger, B. (2007). A paxillin tyrosine phosphorylation switch regulates the assembly and form of cell-matrix adhesions. J. Cell Sci. *120*, 137–148.
40. Geiger, T., and Zaidel-Bar, R. (2012). Opening the floodgates: proteomics and the integrin adhesome. Curr. Opin. Cell Biol. *24*, 562–568.
41. Humphries, J.D., Byron, A., Bass, M.D., Craig, S.E., Pinney, J.W., Knight, D., and Humphries, M.J. (2009). Proteomic analysis of integrin-associated complexes identifies RCC2 as a dual regulator of Rac1 and Arf6. Sci. Signal. *2*, ra51.
42. Kuo, J.C., Han, X., Hsiao, C.T., Yates, J.R., 3rd, and Waterman, C.M. (2011). Analysis of the myosin-II-responsive focal adhesion proteome reveals a role for β-Pix in negative regulation of focal adhesion maturation. Nat. Cell Biol. *13*, 383–393.
43. Oakes, P.W., Beckham, Y., Stricker, J., and Gardel, M.L. (2012). Tension is required but not sufficient for focal adhesion maturation without a stress fiber template. J. Cell Biol. *196*, 363–374.
44. Shutova, M., Yang, C., Vasiliev, J.M., and Svitkina, T. (2012). Functions of nonmuscle myosin II in assembly of the cellular contractile system. PLoS ONE *7*, e40814.
45. Yu, C.H., Law, J.B., Suryana, M., Low, H.Y., and Sheetz, M.P. (2011). Early integrin binding to Arg-Gly-Asp peptide activates actin polymerization and contractile movement that stimulates outward translocation. Proc. Natl. Acad. Sci. USA *108*, 20585–20590.
46. Plotnikov, S.V., Pasapera, A.M., Sabass, B., and Waterman, C.M. (2012). Force fluctuations within focal adhesions mediate ECM-rigidity sensing to guide directed cell migration. Cell *151*, 1513–1527.
47. Breckenridge, M.T., Dulyaninova, N.G., and Egelhoff, T.T. (2009). Multiple regulatory steps control mammalian nonmuscle myosin II assembly in live cells. Mol. Biol. Cell *20*, 338–347.
48. Orr, A.W., Ginsberg, M.H., Shattil, S.J., Deckmyn, H., and Schwartz, M.A. (2006). Matrix-specific suppression of integrin activation in shear stress signaling. Mol. Biol. Cell *17*, 4686–4697.
49. Even-Faitelson, L., and Ravid, S. (2006). PAK1 and aPKCzeta regulate myosin II-B phosphorylation: a novel signaling pathway regulating filament assembly. Mol. Biol. Cell *17*, 2869–2881.
50. Beach, J.R., Hussey, G.S., Miller, T.E., Chaudhury, A., Patel, P., Monslow, J., Zheng, Q., Keri, R.A., Reizes, O., Bresnick, A.R., et al. (2011). Myosin II isoform switching mediates invasiveness after TGF-β-induced epithelial-mesenchymal transition. Proc. Natl. Acad. Sci. USA *108*, 17991–17996.
51. Ludowyke, R.I., Elgundi, Z., Kranenburg, T., Stehn, J.R., Schmitz-Peiffer, C., Hughes, W.E., and Biden, T.J. (2006). Phosphorylation of nonmuscle myosin heavy chain IIA on Ser1917 is mediated by protein kinase C beta II and coincides with the onset of stimulated degranulation of RBL-2H3 mast cells. J. Immunol. *177*, 1492–1499.
52. Edme, N., Downward, J., Thiery, J.P., and Boyer, B. (2002). Ras induces NBT-II epithelial cell scattering through the coordinate activities of Rac and MAPK pathways. J. Cell Sci. *115*, 2591–2601.
53. Hong-Geller, E., and Cerione, R.A. (2000). Cdc42 and Rac stimulate exocytosis of secretory granules by activating the IP(3)/calcium pathway in RBL-2H3 mast cells. J. Cell Biol. *148*, 481–494.
54. Schmitz, A.A., Govek, E.E., Böttner, B., and Van Aelst, L. (2000). Rho GTPases: signaling, migration, and invasion. Exp. Cell Res. *261*, 1–12.